

Data-Driven Bilateral Generalized Two-Dimensional Quaternion Principal Component Analysis with Application to Color Face Recognition

Mei-Xiang Zhao^{a,d}, Zhi-Gang Jia^{b,a,*}, Dun-Wei Gong^{c,*}, Yong Zhang^d

^aSchool of Mathematics and Statistics, Jiangsu Normal University, Xuzhou 221116, P. R. China

^bResearch Institute of Mathematical Science, Jiangsu Normal University, Xuzhou 221116, P. R. China

^cSchool of Information Science and Technology, Qingdao University of Science and Technology, Qingdao, Shandong, 266061, P. R. China

^dSchool of Information and Control Engineering, China University of Mining and Technology, Xuzhou 221116, P. R. China

Abstract

A new data-driven bilateral generalized two-dimensional quaternion principal component analysis (BiG2DQPCA) is presented to extract the features of matrix samples from both row and column directions. This general framework directly works on the 2D color images without vectorizing and well preserves the spatial and color information, which makes it flexible to fit various real-world applications. A generalized ridge regression model of BiG2DQPCA is firstly proposed with orthogonality constraints on aimed features. Applying the deflation technique and the framework of minorization-maximization, a new quaternion optimization algorithm is proposed to compute the optimal features of BiG2DQPCA and a closed-form solution is obtained at each iteration. A new approach based on BiG2DQPCA is presented for color face recognition and image reconstruction with a new data-driven weighting technique. Sufficient numerical experiments are implemented on practical color face databases and indicate the superiority of BiG2DQPCA over the state-of-the-art methods in terms of recognition accuracies and rates of image reconstruction.

Keywords: 2DQPCA, Color face recognition, Quaternion optimization algorithm, data-driven, L_p norm

1. Introduction

Two-dimensional principal component analysis [1] started a history of extracting features of grey image samples without converting them into high-dimensional vectors. With preserving spatial information, these features were firstly taken from eigenvectors corresponding to large eigenvalues of the covariance matrix generated by matrix samples from column direction. Then to obtain features preserving more geometric information, mathematics and scientific scholars developed many powerful variations of 2DPCA by extracting features from row and column directions. However, there are still no 2DPCA-based model with L_p norm to treat color image samples in the literature. In this paper, we develop a new bilateral generalized two-dimensional quaternion principal component analysis with L_p -norm (BiG2DQPCA) to compute features with preserving their spacial and color information.

To recognize color images, it is very important to preserve the cross-channel correlation among red, green and blue channels based on the RGB color space. This correlation is overlooked by the traditional methods which parallelly treat each channel or gather three color channels into a large matrix; see [2, 3] for more advantages of the quaternion representation. Recently, many studies show that purely imaginary quaternion matrices are well adapted to color images by encoding the color channels into three imaginary parts; and the conventional principal component analysis (PCA) and 2DPCA are generalized to quaternion domain, such as the quaternion PCA (QPCA) [4], two-dimensional QPCA (2DQPCA) [5], the bilateral 2DQPCA [6], the kernel QPCA (KQPCA) and the 2DKQPCA [7]. Unfortunately, the non-commutativity of quaternion multiplication makes it impossible to straightforwardly use classic fast algorithms to solve quaternionic (right) eigenproblems and optimization problems. This makes the well

*Corresponding authors

Email addresses: zhgjia@jnsu.edu.cn (Zhi-Gang Jia), dwgong@vip.163.com (Dun-Wei Gong)

developed quaternion variations of PCA and 2DPCA far away from practical application. To overcome the computational difficulty, Jia *et al.*[8] proposed a new version of 2DQPCA, which constrains the features to simultaneously preserve the color and spatial information, and they computed these features in the row direction by the well-known fast structure-preserving algorithms [9, 10]. Xiao *et al.* further presented a mathematically equivalent quaternion ridge regression model for 2DQPCA in [11] and added new sparsity constraints on the features. Then Zhao *et al.* [12] improved 2DQPCA by extracting features from both row and column directions, which saves the storage of compressed samples under feature subspaces and highly lifts the speeds of color face recognition and image reconstruction. These works provide necessary fundamental models and methods for developing new variations of 2DQPCA and quaternion optimization algorithms.

With beautiful geometry and powerful functionality, L_p -norms are playing an increasingly important role in the advanced artificial intelligence models based on principal component analysis (PCA) or 2DPCA. PCA [13] has become a basic method in the computer vision and pattern recognition. To render PCA vulnerable to noises, the quadratic formulation of PCA is improved into L_1 -norm or L_0 -norm on the objection and constrain functions in many sparse and robust models, such as L_1 -PCA [14], R_1 -PCA [15], PCA- L_1 [16], and a series of sparse PCA (SPCA) algorithms [17, 18, 19, 20, 21, 22, 23, 24, 25]. Finally, the generalized PCA (GPCA)[26, 27] uses the L_p -norm on the objective and constraint functions, and extracts features of different geometric properties. In the same period, a plenty of variations of 2DPCA were proposed in the literature, such as 2DPCA- L_1 [28], 2DPCA- L_1 S [29], G2DPCA[30] and many others [31, 32, 33]. Beside, L_p -norms were successfully applied to develop new supervised models, such as the well-known robust bilateral L_p -norm two-dimensional linear discriminant analysis [34]. Motivated by these successful models, we generalize 2DQPCA in [35] to a new bilateral variation with L_p norm. However, L_p -norms of quaternion vectors are still not well defined and let alone their applications. So we need to start our work from the basic definitions and computational methods.

The contributions of this paper are listed in three aspects.

- (1) A new bilateral generalized 2DQPCA with L_p -norm (BiG2DQPCA) is presented with extracting features from both row and column directions. This general framework directly works on the 2D color images without vectorizing and well preserves the spatial and color information, which makes it flexible to fit various real-world applications.
- (2) A generalized ridge regression model of BiG2DQPCA is firstly proposed with adding the orthogonality constrains on aimed features. Applying a deflation technique and the framework of minorization-maximization [36], a new quaternion optimization algorithm is proposed to compute the optimal features of BiG2DQPCA. A closed-form solution is obtained at each step of iteration.
- (3) A new data-driven weighting technique is presented in the BiG2DQPCA approach for color face recognition and image reconstruction. The extracted features are weighted by a learned optimal manner. Sufficient numerical experiments are implemented on practical color face databases to show the data-driven learning of optimal weighting manner and the superiority of BiG2DQPCA over the state-of-the-art methods.

The paper is organized as follows. In Section 2, we define the L_p -norm of quaternion vector and recall two models: 2DQPCA and G2DPCA. In Section 3, we present a new BiG2DQPCA with a new optimization algorithm. In Section 4, we present a BiG2DQPCA approach with a new data-driven technique for color face recognition and image reconstruction. In Section 5, we compare BiG2DQPCA with the advanced variations of 2DPCA in numerical experiments on the GTFD, color FERET, Faces95 and AR databases. Finally, a conclusion and future research topics are proposed in Section 6.

2. Preliminaries

In this section, we present the L_p -norm of quaternion vector and recall two face recognition models (2DQPCA and G2DPCA).

2.1. L_p -norm of quaternion vector

The ring of real quaternions, denoted by

$$\mathbb{H} = \{\mathbf{a} = a_0 + a_1\mathbf{i} + a_2\mathbf{j} + a_3\mathbf{k} \mid a_0, \dots, a_3 \in \mathbb{R}\},$$

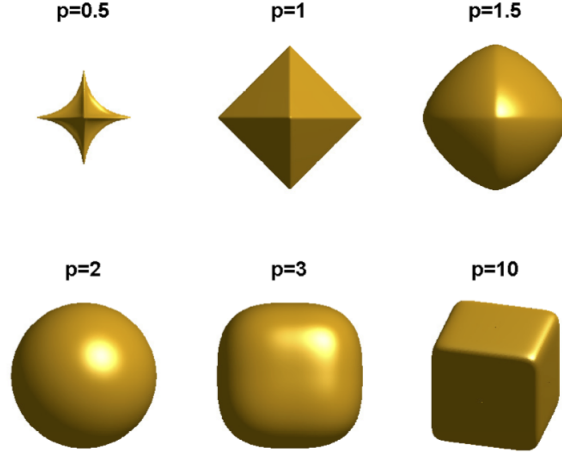


Figure 1: The set of vectors whose L_p norms are less than or equal to one

where three imaginary values \mathbf{i} , \mathbf{j} , \mathbf{k} satisfy $\mathbf{i}^2 = \mathbf{j}^2 = \mathbf{k}^2 = \mathbf{ijk} = -1$, was discovered by Sir William Rowan Hamilton (1805-1865) in 1843. The absolute value and the sign of a quaternion number $\mathbf{a} \in \mathbb{H}$ are defined by

$$|\mathbf{a}| = (|a_0|^2 + |a_1|^2 + |a_2|^2 + |a_3|^2)^{1/2}, \quad (1a)$$

$$\text{sign}(\mathbf{a}) = \begin{cases} \mathbf{a}/|\mathbf{a}|, & \text{if } \mathbf{a} \neq 0, \\ 0, & \text{if } \mathbf{a} = 0. \end{cases} \quad (1b)$$

A quaternion vector $\mathbf{w} \in \mathbb{H}^n$ is of the form

$$\mathbf{w} = [\mathbf{w}_1 \quad \mathbf{w}_2 \quad \cdots \quad \mathbf{w}_n]^T = w^{(0)} + w^{(1)}\mathbf{i} + w^{(2)}\mathbf{j} + w^{(3)}\mathbf{k}$$

where $\mathbf{w}_i = w_i^{(0)} + w_i^{(1)}\mathbf{i} + w_i^{(2)}\mathbf{j} + w_i^{(3)}\mathbf{k}$ denotes the i th entry of \mathbf{w} and $w^{(j)} \in \mathbb{R}^n$, $j = 0, 1, 2, 3$. The sign and the absolute value of \mathbf{w} are defined in the element-wise manner by

$$|\mathbf{w}| = [|\mathbf{w}_1| \quad |\mathbf{w}_2| \quad \cdots \quad |\mathbf{w}_n|]^T, \quad (2a)$$

$$\text{sign}(\mathbf{w}) = [\text{sign}(\mathbf{w}_1) \quad \text{sign}(\mathbf{w}_2) \quad \cdots \quad \text{sign}(\mathbf{w}_n)]^T. \quad (2b)$$

And for zero quaternion vector $\mathbf{v} = 0$, we have $\text{sign}(\mathbf{v}) = 0$. Clearly,

$$\text{sign}(\mathbf{w}) = \begin{bmatrix} \frac{w_1^{(0)}}{|\mathbf{w}_1|} \\ \frac{w_2^{(0)}}{|\mathbf{w}_2|} \\ \vdots \\ \frac{w_n^{(0)}}{|\mathbf{w}_n|} \end{bmatrix} + \begin{bmatrix} \frac{w_1^{(1)}}{|\mathbf{w}_1|} \\ \frac{w_2^{(1)}}{|\mathbf{w}_2|} \\ \vdots \\ \frac{w_n^{(1)}}{|\mathbf{w}_n|} \end{bmatrix} \mathbf{i} + \begin{bmatrix} \frac{w_1^{(2)}}{|\mathbf{w}_1|} \\ \frac{w_2^{(2)}}{|\mathbf{w}_2|} \\ \vdots \\ \frac{w_n^{(2)}}{|\mathbf{w}_n|} \end{bmatrix} \mathbf{j} + \begin{bmatrix} \frac{w_1^{(3)}}{|\mathbf{w}_1|} \\ \frac{w_2^{(3)}}{|\mathbf{w}_2|} \\ \vdots \\ \frac{w_n^{(3)}}{|\mathbf{w}_n|} \end{bmatrix} \mathbf{k}.$$

Given a positive scalar p , we define the L_p norm of quaternion vector \mathbf{w} by

$$\|\mathbf{w}\|_p = \left(\sum_{i=1}^n |\mathbf{w}_i|^p \right)^{\frac{1}{p}}. \quad (3)$$

If $p = 2$, we get the L_2 norm of \mathbf{w} . Note that the L_p norms of quaternion vectors have different geometric properties. See Figure 1 for illustration.

2.2. 2DQPCA

2DQPCA was proposed in [8] for color face recognition. Suppose that an $m \times n$ quaternion matrix is in the form of $\mathbf{Q} = Q_0 + Q_1\mathbf{i} + Q_2\mathbf{j} + Q_3\mathbf{k}$, where $Q_i \in \mathbb{R}^{m \times n}$, $i = 0, 1, 2, 3$. A *pure quaternion matrix* is a matrix whose elements are pure quaternions ($Q_0 = 0$) or zero. In the RGB color space, a color image of size $m \times n$ can be stored by an $m \times n$ pure quaternion matrix $\mathbf{Q} = [\mathbf{q}_{ab}]_{m \times n}$ with each entry $\mathbf{q}_{ab} = r_{ab}\mathbf{i} + g_{ab}\mathbf{j} + b_{ab}\mathbf{k}$ denoting one color pixel, where r_{ab} , g_{ab} and b_{ab} are red, green and blue channels [37].

Suppose that there are ℓ training color image samples in total, denoted as $m \times n$ pure quaternion matrices, $\mathbf{F}_1, \mathbf{F}_2, \dots, \mathbf{F}_\ell$, and the mean image of all the training color images can be defined as follows $\Psi = \frac{1}{\ell} \sum_{i=1}^{\ell} \mathbf{F}_i \in \mathbb{H}^{m \times n}$. Algorithm 1 lists the procedure of 2DQPCA for image recognition. 2DQPCA based on quaternion models can preserve color and spatial information of face images, and its computational complexity of quaternion operations is similar to the computational complexity of real operations of 2DPCA (proposed in [1]).

2.3. G2DPCA

For treating real samples, the generalized two dimensional principal component analysis (G2DPCA) was proposed in [30] by using L_p -norm in both the objective function and the constraint function.

Suppose that $F_1, F_2, \dots, F_\ell \in \mathbb{R}^{m \times n}$ are ℓ real samples and they are centralized, that is, $\sum_{i=1}^{\ell} F_i = 0$. G2DPCA solves the following optimization function

$$\max_w \sum_{i=1}^{\ell} \|F_i w\|_s^s, \text{ s.t. } \|w\|_p^p = 1,$$

where $w \in \mathbb{R}^n$, $s \geq 1$, and $p > 0$. In [30], an iterative algorithm is designed to solve the optimization problem of G2DPCA under the minorization-maximization (MM) framework [36], and a closed-form solution is obtained in each iteration. The solution of G2DPCA is guaranteed to be locally optimal.

Algorithm 1 2DQPCA: Two dimensional quaternion principal component analysis

- 1: Compute the following *color image covariance matrix* of training samples $\mathbf{G}_t = \frac{1}{\ell} \sum_{i=1}^{\ell} (\mathbf{F}_i - \Psi)^* (\mathbf{F}_i - \Psi) \in \mathbb{H}^{m \times n}$, where $\Psi = \frac{1}{\ell} \sum_{i=1}^{\ell} \mathbf{F}_i$.
 - 2: Compute the k ($1 \leq k \leq n$) largest eigenvalues of \mathbf{G}_t and their corresponding eigenvectors (called eigenfaces), denoted as $(\lambda_1, \mathbf{w}_1), \dots, (\lambda_k, \mathbf{w}_k)$. Let the eigenface subspace be $\mathbf{W} = \text{span}\{\mathbf{w}_1, \dots, \mathbf{w}_k\}$.
 - 3: Compute the projections of ℓ training color face images in the subspace \mathbf{W} , $\mathbf{P}_i = (\mathbf{F}_i - \Psi)\mathbf{W} \in \mathbb{H}^{m \times k}$, $i = 1, \dots, \ell$.
 - 4: For a given testing sample, \mathbf{F} , compute its feature matrix, $\mathbf{P} = (\mathbf{F} - \Psi)\mathbf{W}$. Seek the nearest face image, \mathbf{F}_i ($1 \leq i \leq \ell$), whose feature matrix satisfies that $\|\mathbf{P}_i - \mathbf{P}\| = \min$. \mathbf{F}_i is output as the person to be recognized.
-

3. Bilateral Generalized 2DQPCA

In this section, we present a bilateral generalized 2DQPCA (BiG2DQPCA) with a generalized regression ridge model and a new quaternion optimization algorithm.

3.1. Generalized ridge regression model

Suppose that $\mathbf{F}_1, \mathbf{F}_2, \dots, \mathbf{F}_\ell \in \mathbb{H}^{m \times n}$, are ℓ quaternion matrix samples and they are assumed to be mean-centered, i.e., $\Psi := \frac{1}{\ell} \sum_{i=1}^{\ell} \mathbf{F}_i = 0$; otherwise, define $\mathbf{F}_i := \mathbf{F}_i - \Psi$ for $i = 1, \dots, \ell$. The generalized ridge regression model of BiG2DQPCA is

$$\begin{aligned} \begin{pmatrix} \widehat{\mathbf{u}}_1, \dots, \widehat{\mathbf{u}}_{k_1}, \\ \widehat{\mathbf{v}}_1, \dots, \widehat{\mathbf{v}}_{k_2} \end{pmatrix} &= \arg \max_{\mathbf{u}_{j_1} \in \mathbb{H}^{n_1}, \mathbf{v}_{j_2} \in \mathbb{H}^{n_2}} \sum_{i=1}^{\ell} \left(\sum_{j_1=1}^{k_1} \|\mathbf{u}_{j_1}^* \mathbf{F}_i\|_s^s + \sum_{j_2=1}^{k_2} \|\mathbf{F}_i \mathbf{v}_{j_2}\|_s^s \right), \\ \text{s.t. } \|\mathbf{u}_j\|_p &= 1, \mathbf{u}_j^* \mathbf{u}_i = 0, i \neq j, i, j = 1, 2, \dots, k_1, \\ \|\mathbf{v}_j\|_p &= 1, \mathbf{v}_j^* \mathbf{v}_i = 0, i \neq j, i, j = 1, 2, \dots, k_2, \end{aligned} \quad (4)$$

where $s \geq 1, p > 0$, and k_1, k_2 are two given positive integers. In this new model, L_p -norms are used in both the objective function and the constraint function. The constraints $\|\mathbf{u}_j\|_p \leq 1$ and $\|\mathbf{v}_j\|_p \leq 1$ are convex if $p \geq 1$ and non-convex if $0 < p < 1$.

Especially, if $s = p = 2$, then BiG2DQPCA reduces to a bilateral two dimensional quaternion component analysis (Bi2DQPCA), which is not proposed in the literature. Such Bi2DQPCA can be modelled in a matrix form. Define $\mathbf{U}_{k_1} = [\mathbf{u}_1, \dots, \mathbf{u}_{k_1}]$ and $\mathbf{V}_{k_2} = [\mathbf{v}_1, \dots, \mathbf{v}_{k_2}]$. Applying the Frobenius norm (F-norm), Bi2DQPCA can be rewritten into

$$\begin{aligned} (\widehat{\mathbf{U}}_{k_1}, \widehat{\mathbf{V}}_{k_2}) &= \arg \max_{\mathbf{U}_{k_1}, \mathbf{V}_{k_2}} \sum_{i=1}^{\ell} \left(\|\mathbf{U}_{k_1}^* \mathbf{F}_i\|_F^2 + \|\mathbf{F}_i \mathbf{V}_{k_2}\|_F^2 \right), \\ \text{s.t. } \mathbf{U}_{k_1}^* \mathbf{U}_{k_1} &= I_{k_1}, \quad \mathbf{V}_{k_2}^* \mathbf{V}_{k_2} = I_{k_2}. \end{aligned} \quad (5)$$

Moreover, from the constrains that the columns of \mathbf{U}_{k_1} and \mathbf{V}_{k_2} are orthonormal, we observe that

$$\|\mathbf{U}_{k_1}^* \mathbf{F}_i\|_F^2 = \text{trace}(\mathbf{F}_i^* \mathbf{U}_{k_1} \mathbf{U}_{k_1}^* \mathbf{F}_i) = \|\mathbf{U}_{k_1} \mathbf{U}_{k_1}^* \mathbf{F}_i\|_F^2$$

and

$$\|\mathbf{F}_i \mathbf{V}_{k_2}\|_F^2 = \text{trace}(\mathbf{F}_i \mathbf{V}_{k_2} \mathbf{V}_{k_2}^* \mathbf{F}_i^*) = \|\mathbf{F}_i \mathbf{V}_{k_2} \mathbf{V}_{k_2}^*\|_F^2.$$

Then the matrix form of Bi2DQPCA is mathematically equivalent to

$$\begin{aligned} (\widehat{\mathbf{U}}_{k_1}, \widehat{\mathbf{V}}_{k_2}) &= \arg \min_{\mathbf{U}_{k_1}, \mathbf{V}_{k_2}} \sum_{i=1}^{\ell} \left(\|\mathbf{F}_i - \mathbf{U}_{k_1} \mathbf{U}_{k_1}^* \mathbf{F}_i\|_F^2 + \|\mathbf{F}_i - \mathbf{F}_i \mathbf{V}_{k_2} \mathbf{V}_{k_2}^*\|_F^2 \right), \\ \text{s.t. } \mathbf{U}_{k_1}^* \mathbf{U}_{k_1} &= I_{k_1}, \quad \mathbf{V}_{k_2}^* \mathbf{V}_{k_2} = I_{k_2}. \end{aligned} \quad (6)$$

Remark that BiG2DQPCA of form (4) is a novel and general model that covers many well-known 2DPCA-based models. Firstly, BiG2DQPCA is a generalization of G2DPCA [30] from the real field to the quaternion skew-field and from one-directional feature extraction to two-directional feature extraction. Compared with G2DPCA, we firstly constrain the orthogonality of the projection vectors, $\mathbf{w}_i, i = 1, 2, \dots, r$, in the ridge regression model (4). Secondly, BiG2DQPCA also generalizes 2DQPCA [12] by applying L_p -norm in both the objective function and the constraint function. Thirdly, in the special case that $s = p = 2$, Bi2DQPCA of the matrix form (6) is a generalization of the QRR model [11] from one-directional model to bilateral model.

3.2. Quaternion optimization algorithm

Now we present a new quaternion optimization algorithm of BiG2DQPCA by solving the generalized ridge regression model (4). The pseudocode based on quaternion domain is given in Algorithm 2. For simplicity of expression, we define \odot by multiplying a real vector to a quaternion vector: Let $w \in \mathbb{R}^n$ and $\mathbf{v} = v_0 + v_1\mathbf{i} + v_2\mathbf{j} + v_3\mathbf{k} \in \mathbb{H}^n$, then

$$w \odot \mathbf{v} = (w \circ v_0) + (w \circ v_1)\mathbf{i} + (w \circ v_2)\mathbf{j} + (w \circ v_3)\mathbf{k},$$

where \circ denotes the Hadamard product of two real vectors. In the practical computation we realize quaternion operations by the real structure-preserving method firstly proposed in [9]. The real representations of quaternion matrix $\mathbf{F} = F_0 + F_1\mathbf{i} + F_2\mathbf{j} + F_3\mathbf{k} \in \mathbb{H}^{m \times n}$ and quaternion vector $\mathbf{w} \in \mathbb{H}^n$ are defined by

$$\mathbf{F}^{(\Upsilon)} \equiv \begin{bmatrix} F_0 & -F_1 & -F_2 & -F_3 \\ F_1 & F_0 & -F_3 & F_2 \\ F_2 & F_3 & F_0 & -F_1 \\ F_3 & -F_2 & F_1 & F_0 \end{bmatrix} \in \mathbb{R}^{4m \times 4n},$$

$$\mathbf{w}^{(\Upsilon)} \equiv \begin{bmatrix} (w^{(0)})^T & (w^{(1)})^T & (w^{(2)})^T & (w^{(3)})^T \end{bmatrix}^T \in \mathbb{R}^{4n}.$$

The quaternion matrix-vector product $\mathbf{y} = \mathbf{F}\mathbf{w}$ is equivalent to the real matrix-vector product $\mathbf{y}^{(\Upsilon)} = \mathbf{F}^{(\Upsilon)}\mathbf{w}^{(\Upsilon)}$.

In Algorithm 2, the deflation technique is applied to provide a proper searching subspace for computing the next principal component once the former ones have been obtained. Assume that the first k_1 left projectors and the first k_2

Algorithm 2 BiG2DQPCA: Bilateral generalized two dimensional quaternion principal component analysis with L_p norm

Require: Training samples $\mathbf{F}_1, \mathbf{F}_2, \dots, \mathbf{F}_\ell$, two positive integers k_1 and k_2 , and parameters $s \in [1, \infty), p \in (0, \infty]$.

Ensure: Optimal quaternion projection matrices \mathbf{U} and \mathbf{V} , and weighted coefficient matrices D^{left} and D^{right} .

- 1: Initialize $\mathbf{U} = [\]$, $D^{left} = [\]$, $\mathbf{V} = [\]$, $D^{right} = [\]$, $\mathbf{F}_i^{left} = \mathbf{F}_i^{right} = \mathbf{F}_i$.
 - 2: **for** $t = 1, 2, \dots, k_2$ **do**
 - 3: Initialize $k = 0$, $\delta = 1$, arbitrary \mathbf{w}^0 with $\|\mathbf{w}^0\|_p = 1$, and $f^0 = \sum_{i=1}^{\ell} \|\mathbf{F}_i^{right} \mathbf{w}^0\|_s$.
 - 4: **while** $\delta > 10^{-4}$ **do**
 - 5: $\mathbf{y}^k = \sum_{i=1}^{\ell} (\mathbf{F}_i^{right})^* [|\widehat{\mathbf{w}}^k|^{s-1} \odot \text{sign}(\widehat{\mathbf{w}}^k)]$, where $\widehat{\mathbf{w}}^k = \mathbf{F}_i^{right} \mathbf{w}^k$.
 - 6: **if** $0 < p < 1$ **then**
 - 7: $\mathbf{y}^k = |\mathbf{w}^0| \odot |\mathbf{w}^k|^{1-p} \odot \mathbf{y}^k$, $\mathbf{w}^{k+1} = \mathbf{y}^k / \|\mathbf{y}^k\|_p$.
 - 8: **else if** $p = 1$ **then**
 - 9: $j = \underset{i \in [1, n]}{\text{argmax}} |\mathbf{y}_i^k|$, $\mathbf{w}_i^{k+1} = \begin{cases} \text{sign}(\mathbf{y}_j^k), & i = j, \\ 0, & i \neq j. \end{cases}$
 - 10: **else if** $1 < p < \infty$ **then**
 - 11: $q = p/(p-1)$, $\mathbf{y}^k = |\mathbf{y}^k|^{q-1} \odot \text{sign}(\mathbf{y}^k)$, $\mathbf{w}^{k+1} = \mathbf{y}^k / \|\mathbf{y}^k\|_p$.
 - 12: **else if** $p = \infty$ **then**
 - 13: $\mathbf{w}^{k+1} = \text{sign}(\mathbf{y}^k)$.
 - 14: **end if**
 - 15: $f^{k+1} = \sum_{i=1}^{\ell} \|\mathbf{F}_i^{right} \mathbf{w}^{k+1}\|_s$, $\delta = |f^{k+1} - f^k|/|f^k|$.
 - 16: $k \leftarrow k + 1$.
 - 17: **end while**
 - 18: $\mathbf{v}^t = \mathbf{w}^k$.
 - 19: Orthogonalize \mathbf{v}^t with the previous vectors $\mathbf{v}_1, \dots, \mathbf{v}_{t-1}$ by quaternion QR decomposition.
 - 20: $f^t = \sum_{i=1}^{\ell} \|\mathbf{F}_i^{right} \mathbf{v}^t\|_s$, $\mathbf{V} \leftarrow [\mathbf{V}, \mathbf{v}^t]$, $D^{right} = [D^{right}, f^t]$.
 - 21: $\mathbf{F}_i^{right} \leftarrow \mathbf{F}_i^{right} (\mathbf{I} - \mathbf{V}\mathbf{V}^*)$, $i = 1, 2, \dots, \ell$.
 - 22: **end for**
 - 23: Run from steps 2-30 again with replacing k_2 with k_1 , $\mathbf{F}_i \mathbf{w}^k$ with $(\mathbf{w}^k)^* \mathbf{F}_i$, \mathbf{v}^t with \mathbf{u}^t , \mathbf{V} with \mathbf{U} , \mathbf{F}_i^{right} with \mathbf{F}_i^{left} , D^{right} with D^{left} , and $\mathbf{F}_i^{right} (\mathbf{I} - \mathbf{V}\mathbf{V}^*)$ with $(\mathbf{I} - \mathbf{U}\mathbf{U}^*) \mathbf{F}_i^{left}$, respectively.
-

right projectors have been computed, and define $\mathbf{U}_{k_1} = [\mathbf{u}_1, \mathbf{u}_2, \dots, \mathbf{u}_{k_1}]$ and $\mathbf{V}_{k_2} = [\mathbf{v}_1, \mathbf{v}_2, \dots, \mathbf{v}_{k_2}]$, where $1 \leq k_1 < m$ and $1 \leq k_2 < n$. The next projectors \mathbf{u}_{k_1+1} and \mathbf{v}_{k_2+1} could be calculated similarly on the deflated samples

$$\mathbf{F}_i^{left} = (\mathbf{I} - \mathbf{U}\mathbf{U}^*)\mathbf{F}_i, \quad \mathbf{F}_i^{right} = \mathbf{F}_i(\mathbf{I} - \mathbf{V}\mathbf{V}^*), \quad (7)$$

where $i = 1, 2, \dots, \ell$. What is particularly noteworthy is that the additional projection vector \mathbf{u}_{k_1+1} (or \mathbf{v}_{k_2+1}) obtained at each iteration must be orthonormalized against all previous projection vectors by the modified Gram-Schmidt procedure in the quaternion domain. The reason is that once we complete deflation in the known directions, there is no information left in these directions and thus, the new projection on the deflated samples should be zero. We observe that after $(k_1 + k_2)$ steps each sample is transformed into two deflated samples as in (7). That is, if samples are projected into the first k_1 directions then

$$\mathbf{u}_j^*(\mathbf{I} - \mathbf{U}\mathbf{U}^*)\mathbf{F}_i = 0, \quad j = 1, \dots, k_1, \quad (8a)$$

$$\mathbf{F}_i(\mathbf{I} - \mathbf{V}\mathbf{V}^*)\mathbf{v}_j = 0, \quad j = 1, \dots, k_2. \quad (8b)$$

If (8) does not hold, then the feature information can be lost because of the interference from other directions. From (8), we also know that the next projector can not be linearly represented by the prior projectors, in other words, the newly computed projector is not included in the subspace generated by the known projectors. So that we orthogonalize the computed projector to the known ones.

4. Color face recognition with data-driven weighting

In this section, we present a new BiG2DQPCA approach for color face recognition and reconstruction. A new data-driven weighting technique is proposed.

At first, we consider how to weight the computed projections. The objective function values corresponding to the optimal projection vectors $\mathbf{u}_1, \dots, \mathbf{u}_{k_1}$ and $\mathbf{v}_1, \dots, \mathbf{v}_{k_2}$ are respectively computed by

$$f^{left}(k_1) = \sum_{i=1}^n \left(\sum_{j_1=1}^{k_1} \|\mathbf{u}_{j_1}^* \mathbf{F}_i\|_s^s \right), \quad f^{right}(k_2) = \sum_{i=1}^n \left(\sum_{j_2=1}^{k_2} \|\mathbf{F}_i \mathbf{v}_{j_2}\|_s^s \right).$$

Naturally, the increments

$$w^{left}(k_1) = f^{left}(k_1) - f^{left}(k_1 - 1), \quad w^{right}(k_2) = f^{right}(k_2) - f^{right}(k_2 - 1)$$

characterize the contributions of \mathbf{u}_{k_1} and \mathbf{v}_{k_2} to the objective function, and thus can be seen as their weighting factors, respectively. Then the joint weighting factor of the pair $(\mathbf{u}_{k_1}, \mathbf{v}_{k_2})$ is directly defined by $w(k_1, k_2) = w^{left}(k_1) + w^{right}(k_2)$. From now on, we denote the left eigenface subspace of BiG2DQPCA by $\mathbf{U} = [\mathbf{u}_1, \dots, \mathbf{u}_{k_1}]$ and the right eigenface subspace by $\mathbf{V} = [\mathbf{v}_1, \dots, \mathbf{v}_{k_2}]$. Their weighting vectors are defined by $\mathbf{W}^{left} = \text{Diag}([w^{left}(1), \dots, w^{left}(k_1)])$ and $\mathbf{W}^{right} = \text{Diag}([w^{right}(1), \dots, w^{right}(k_2)])$.

Under the assumption that all training samples are centralized, i.e., $\Psi = 0$, the weighted projections of ℓ training face images on the subspaces \mathbf{U} and \mathbf{V} are defined by

$$\mathbf{P}_i = (\mathbf{U}\mathbf{W}^{left})^* \mathbf{F}_i (\mathbf{V}\mathbf{W}^{right}) \in \mathbb{H}^{k_1 \times k_2}, \quad (9)$$

where $i = 1, \dots, \ell$. Such \mathbf{P}_i is called the *feature matrix* or *feature image* of the sample image \mathbf{F}_i . In the experiments we use the 1-nearest neighbour (1NN) for the recognition with the feature matrix. In Algorithm 3, we present a new BiG2DQPCA approach with weighted projection for color image recognition.

In the practical face recognition tasks, we find the importances of features in row and column directions are not equal to each other and the manner of weighting relies on the data. To improve the efficiency of recognition, we replace the fixed weighting manner in (9) by a new data-driven weighting technique.

Let $f(\mathbf{W}^{left})$ and $f(\mathbf{W}^{right})$ be the functions of \mathbf{W}^{left} and \mathbf{W}^{right} . Four alternative weighting methods are given as follows.

(1) Unweighted projection of face image \mathbf{F}_i on the subspaces \mathbf{U} and \mathbf{V} , i.e.,

$$\mathbf{P}_i = \mathbf{U}^* \mathbf{F}_i \mathbf{V} \in \mathbb{H}^{k_1 \times k_2}.$$

(2) Left-weighted projection of face image \mathbf{F}_i on the subspaces \mathbf{U} and \mathbf{V} , i.e.,

$$\mathbf{P}_i = (\mathbf{U} f(\mathbf{W}^{left}))^* \mathbf{F}_i (\mathbf{V}) \in \mathbb{H}^{k_1 \times k_2}.$$

(3) Right-weighted projection of face image \mathbf{F}_i on the subspaces \mathbf{U} and \mathbf{V} , i.e.,

$$\mathbf{P}_i = (\mathbf{U})^* \mathbf{F}_i (\mathbf{V} f(\mathbf{W}^{right})) \in \mathbb{H}^{k_1 \times k_2}.$$

(4) Bilateral weighted projection of face image \mathbf{F}_i on the subspaces \mathbf{U} and \mathbf{V} , i.e.,

$$\mathbf{P}_i = (\mathbf{U} f(\mathbf{W}^{left}))^* \mathbf{F}_i (\mathbf{V} f(\mathbf{W}^{right})) \in \mathbb{H}^{k_1 \times k_2}.$$

Algorithm 3 BiG2DQPCA with weighted projection for image recognition

- 1: For mean-centered training samples \mathbf{F}_i , $i = 1, 2, \dots, \ell$, compute the k_1 left and k_2 right ($1 \leq k_1 \leq m$, $1 \leq k_2 \leq n$) projection vectors and their corresponding weighting vectors by Algorithm 2, denoted by (\mathbf{U}, D^{left}) and (\mathbf{V}, D^{right}) .
- 2: Let $\mathbf{W}^{left} = \text{Diag}(D^{left})$ and $\mathbf{W}^{right} = \text{Diag}(D^{right})$. Compute the projections of ℓ training color face images

$$\mathbf{P}_i = (\mathbf{U} \mathbf{W}^{left})^* \mathbf{F}_i (\mathbf{V} \mathbf{W}^{right}) \in \mathbb{H}^{k_1 \times k_2}, \quad i = 1, \dots, \ell.$$

- 3: For a given testing sample, \mathbf{F} , compute its feature matrix, $\mathbf{P} = (\mathbf{U} \mathbf{W}^{left})^* \mathbf{F} (\mathbf{V} \mathbf{W}^{right})$. Seek the nearest face image, \mathbf{F}_i ($1 \leq i \leq \ell$), whose feature matrix satisfies that $i = \arg \min_j \|\mathbf{P}_j - \mathbf{P}\|$. \mathbf{F}_i is output as the person to be recognized.
-

Now the question becomes which manner of weighting and what function f should we choose. The answer is to make a choice with relying on the property of the obtained data. Let D denote the training set of samples and T the test set. We randomly select two mutually exclusive sets from D : one is seen as a new training set S and another is used as the validation set V . Then we train BiG2DQPCA with four weighting formulae on S , and test the recognition rate on V . In general, we repeat the random selection and the training-testing process for several times, and then take the average values as the evaluation results, which help us to make a decision on the final weighting manner. In our experiments, we repeat the whole process for three times and report the average results as the selection criteria. Once the weighting manner is decided, BiG2DQPCA is retrained with the original training set D . The flowchart of BiG2DQPCA with data-driven weighting is illustrated in Figure 2.

We close this section by applying BiG2DQPCA to color image reconstruction. Once the subspace and the projections are computed by Algorithm 2, all we need is to project the projections of image samples back into the subspace. The reconstruction process is described in Algorithm 4. Let \mathbf{F}_i^{rec} be the computed approximation to \mathbf{F}_i , $i = 1, \dots, \ell$. Then the ratio of image reconstruction is defined by

$$Ratio = \frac{1}{\ell} \sum_{i=1}^{\ell} \left(1 - \frac{\|\mathbf{F}_i - \mathbf{F}_i^{rec}\|_F}{\|\mathbf{F}_i\|_F} \right). \quad (10)$$

5. Experiments

In this section, we evaluate the proposed BiG2DQPCA model on three face databases:

- GTFD—The Georgia Tech face database (GTFD)¹ contains 750 images from 50 subjects, fifteen images per subject. It includes various pose faces with various expressions on cluttered backgrounds. All the images are manually cropped, and then resized to 44×33 pixels. Some cropped images are shown in Figure 3.

¹http://www.anefian.com/research/face_reco.htm.

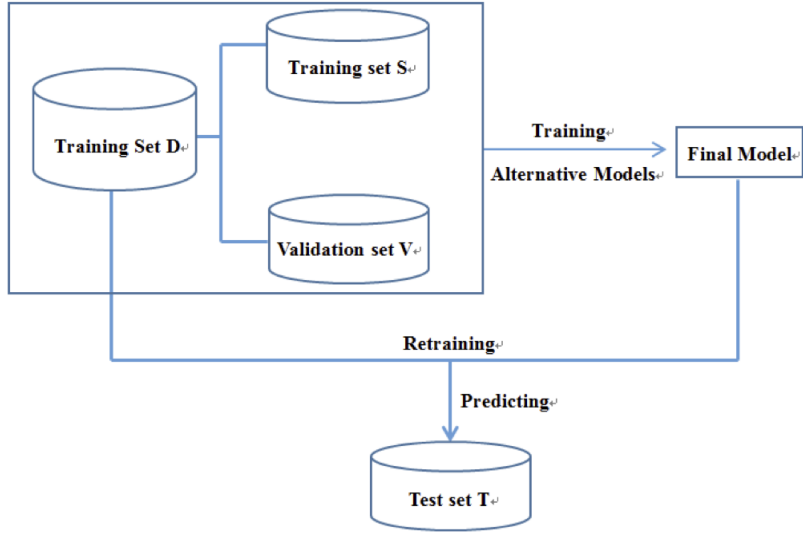


Figure 2: Flowchart of BiG2DQPCA with data-driven weighting for face recognition

Algorithm 4 BiG2DQPCA for color image reconstruction

- 1: For the mean-centered given training samples \mathbf{F}_i , $i = 1, 2, \dots, \ell$, compute the left k_1 and right k_2 ($1 \leq k_1 \leq n$, $1 \leq k_2 \leq n$) projection vectors by Algorithm 2, denoted as $(\mathbf{U}, \mathbf{W}^{left})$ and $(\mathbf{V}, \mathbf{W}^{right})$.
- 2: Add the average image of all training samples then

$$\mathbf{F}_i^{rec} = \mathbf{U}(\mathbf{W}^{left})^{-1} \mathbf{P}_i (\mathbf{W}^{right})^{-1} \mathbf{V}^*. \quad (11)$$

is output as the image to be reconstructed.



Figure 3: Sample color face images from the Georgia Tech face database.

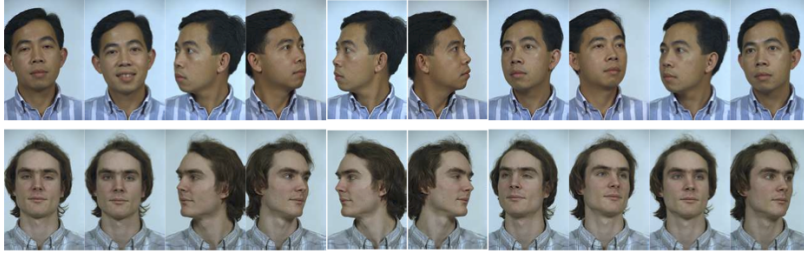


Figure 4: Sample color face images from the color Feret database.

- ColorFeret—The color FERET database² contains 1199 persons, 14126 color face images, and each person has various numbers of face images with various backgrounds. The minimal number of face images for one person is 6, and the maximal one is 44. The size of each cropped color face image is 192×128 pixels. Here we take 11 images of 275 individuals as an example. Some samples occluded with noise are shown in Figure 4.
- Faces95—Faces95 database³ contains 1440 images photographed over a uniform background from 72 subjects and 20 images per subject. The size of each color face image is 200×180 pixels. Some samples are displayed in Figure 5.
- AR—AR face database⁴ contains frontal color face images of 126 people recorded in two sessions. In each session, a neutral color face image is followed by images with different expressions and illumination, and images occluded by sunglasses and scarf (three images per condition). We employ a popular subset of AR containing 100 subjects without occlusion, and hence, 1400 images in total are used. Sample images from AR are given in Figure 6.

The numerical experiments are to test the efficiencies of the methods in the task of image reconstruction and recognition with or without noise. We firstly compare the effects of four different weighting methods on the recognition results, then select the best weighting methods for face databases. As mentioned in Section 4, the weighting vectors for \mathbf{U} and \mathbf{V} are denoted by \mathbf{W}^{left} and \mathbf{W}^{right} , respectively. Here we consider four cases: the projection matrices are not weighted (Unweighted), only \mathbf{U} is weighted by \mathbf{W}^{left} on the left (Weighted Left), only \mathbf{V} is weighted by \mathbf{W}^{right} on the right (Weighted Right), and both \mathbf{U} and \mathbf{V} are weighted by \mathbf{W}^{left} and \mathbf{W}^{right} on the left and the right (Weightd Left and Right), respectively. For each database, we randomly select 3 splits into 80% training, 10% validation and 10% test images. The parameters are optimized on the validation set and tested on the test set.

²<https://www.nist.gov/itl/iad/image-group/color-feret-database>.

³<https://cswwww.essex.ac.uk/mv/allfaces/faces95.html>.

⁴<https://www2.ece.ohio-state.edu/~aleix/ARdatabase.html>.



Figure 5: Sample color face images from the faces95 database.



Figure 6: Sample color face images from the AR database.

Example 5.1 (Weighting Manner Selection). We firstly proceed to investigate the recognition performance on all four databases with different weighting methods. In this weight training process, the parameters s and p are fixed to $s = 2$ and $p = 2$. The function f of \mathbf{W}^{left} and \mathbf{W}^{right} is set as $f(\mathbf{W}) = \mathbf{W}$. The whole procedure is repeated three times and the average recognition rate is reported. Figures 7 and 8 show the average recognition accuracy with four weighting manners on all the databases. The numbers of the chosen eigenfaces in the column direction are shown in X axes and the numbers of the chosen eigenfaces in the row direction are shown in Y axes.

As a special case, we select the same numbers of the eigenfaces in both row and column directions. And the recognition rates on validation set of four different databases are shown in Figure 9. Here we notice that for AR database, the other three weighting methods seem not effectively compared with the unweighted case. So we try to take $f(\mathbf{W}) = 1/\log(\mathbf{W})$ and the results are shown in Figure 10. The pictures display that for AR database, the projections with two-side weighting vectors achieve the highest classification accuracy if we select $f(\mathbf{W}) = 1/\log(\mathbf{W})$.

To further verify the reliability of the selected weighting method, we then test the rotated pictures of all databases. Some rotated samples are shown in Figure 11. Figure 12 displays that for the rotated GTFD, Faces95 and Color FERET databases, the projections with left weighting vectors achieve the highest recognition accuracy.

Example 5.2 (Color Face Recognition). In this example, we proceed to investigate the recognition performance of BiG2DQPCA (Algorithm 3) and compare the results with several leading methods, including 2DPCA [1], QPCA [4], 2DQPCA [5], G2DPCA [30] and QRR [11]. For GTFD, Faces95 and Color Feret databases, the weighting model chosen in the last experiment is the projection matrix \mathbf{V} weighted by $f(\mathbf{W}^{right}) = \mathbf{W}^{right}$ on the right, that is, for a face image \mathbf{F} , its projection \mathbf{P} equals to $\mathbf{U}^* \mathbf{F} (\mathbf{V} f(\mathbf{W}^{right}))$. For AR database, the weighting model is chosen as the projection matrices \mathbf{U} and \mathbf{V} are both weighted by $f(\mathbf{W}^{left})$ and $f(\mathbf{W}^{right})$ on left and right and the function f is selected as $f(\mathbf{W}) = 1/\log(\mathbf{W})$. For simplicity, let $w(s, p)$ denote BiG2DQPCA with L_s -norm and L_p -norm in all figures. Figure 13 shows the recognition accuracies of BiG2DQPCA with different parameter pairs $w(s, p)$ on four databases. The results indicate that the optimal parameter pair (s, p) relies on the databases. Table 1 presents the best recognition rates on different databases and their corresponding optimal parameter pairs (s, p) .

The following experiments compare the recognition accuracies of different algorithms on the color face images where the parameter pairs (s, p) for BiG2DQPCA are set as those shown in Table 1. Figure 14 illustrates the comparison results.

Example 5.3 (Color Image Reconstruction). In this example, we apply BiG2DQPCA (Algorithm 4) to reconstruct the color face images in training set from their projections. The setting is as follows. For GTFD database, the number

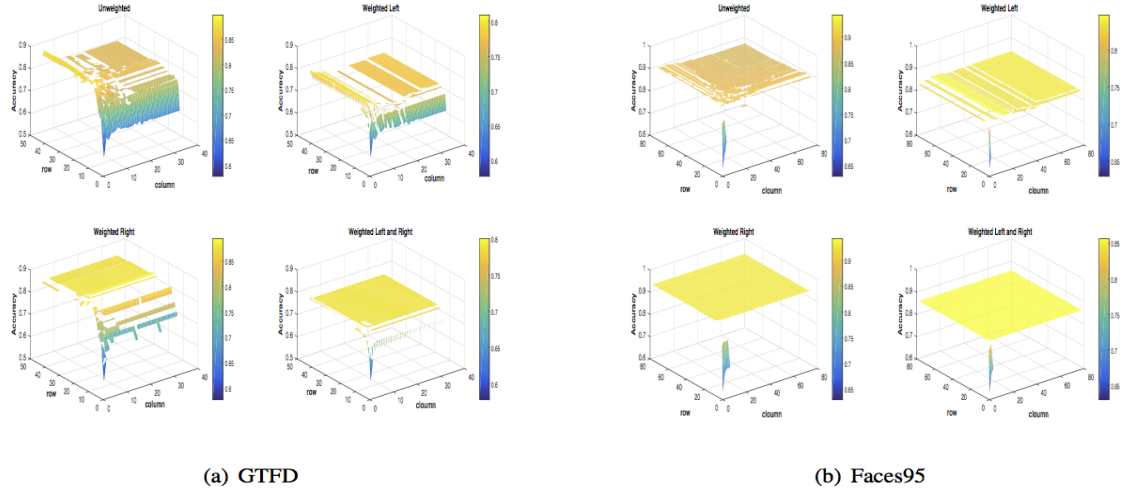


Figure 7: Recognition accuracies of BiG2DQPCA with four different weighing method on the GTFD(left) and Faces95(right) validation sets.

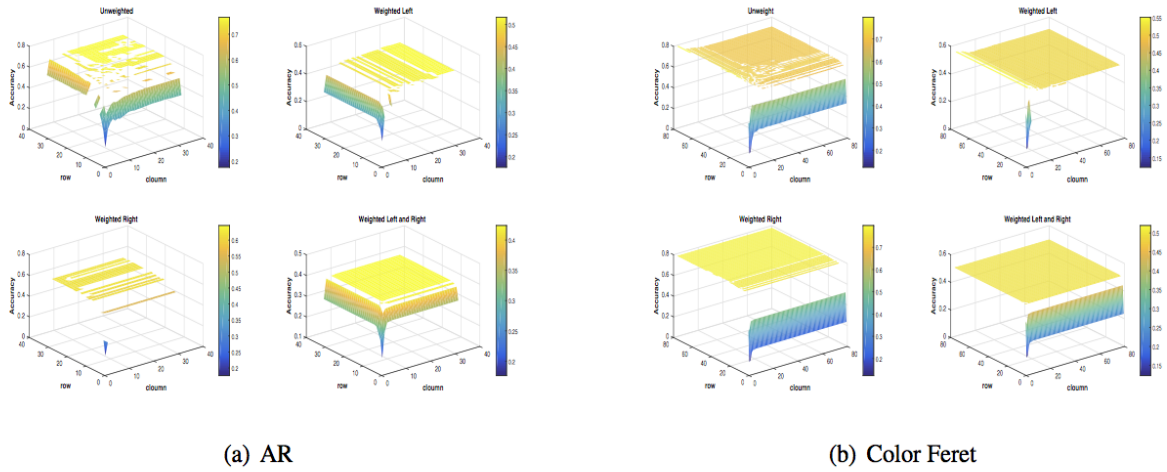


Figure 8: Recognition accuracies of BiG2DQPCA with four different weighing methods on the AR(left) and Color Feret(right) validation sets.

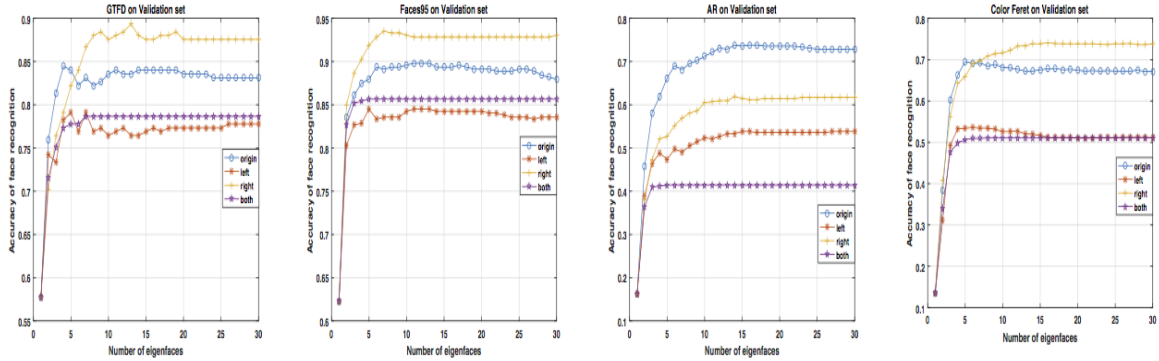


Figure 9: Recognition accuracies of BiG2DQPCA with four different weighing method on the GTFD, Faces95, AR and Color Feret validation sets. The numbers of the chosen eigenfaces are all from 1 to 30.

Table 1: Optimal Parameter Pair (s, p) on Four Databases

Database	Optimal parameters	Accuracy
GTFD	$s=2, p=0.5$	93.33%
Faces95	$s=2, p=2$	96.53%
Color Feret	$s=2, p=\text{inf}$	80.20%
AR	$s=2, p=2$	85.00%

of eigenfaces changes from 1 to 44 and 1 to 33 in row space and column space, respectively. For AR database, the number of eigenfaces changes from 1 to 32 in both row direction and column direction. And for Color Feret and Faces95 databases, the number of eigenfaces changes from 1 to 80 in both row space and column space. In Figure 15, we plot the ratios of image reconstruction defined by (10) on four databases. These results indicate that the BiG2DQPCA is convenient to reconstruct color face images from projections, and can reconstruct original color face images with choosing all the eigenvectors to span the eigenface subspace.

6. Conclusion and future works

In this paper, a novel BiG2DQPCA is presented for color face recognition and image reconstruction based on quaternion models. This general model generalizes famous 2DPCA-like methods, such as 2DPCA- L_1 , Bi2DPCA and G2DPCA, from real field to quaternion ring, and also generalizes 2DQPCA from L_2 -norm constrain to L_p -norm constrain. In addition, BiG2DQPCA extracts features of 2D color image samples from both row and column directions, and weights them by a new data-driven weighting technique. The numerical experiments on the widely used face databases (GTFD, Faces 95, AR, and color Feret) indicate the superiority of BiG2DQPCA over the state-of-the-art methods.

In the future, we will study a data-driven method of searching optimal L_s -norm and L_p -norm in the BiG2DQPCA model and apply BiG2DQPCA to solve other color imaging problems, such as color image semantic segmentation and medical image processing. We will also consider generalizing the two-dimensional linear discriminant analysis models in [38, 39, 40, 41] to new variations with L_p norm.

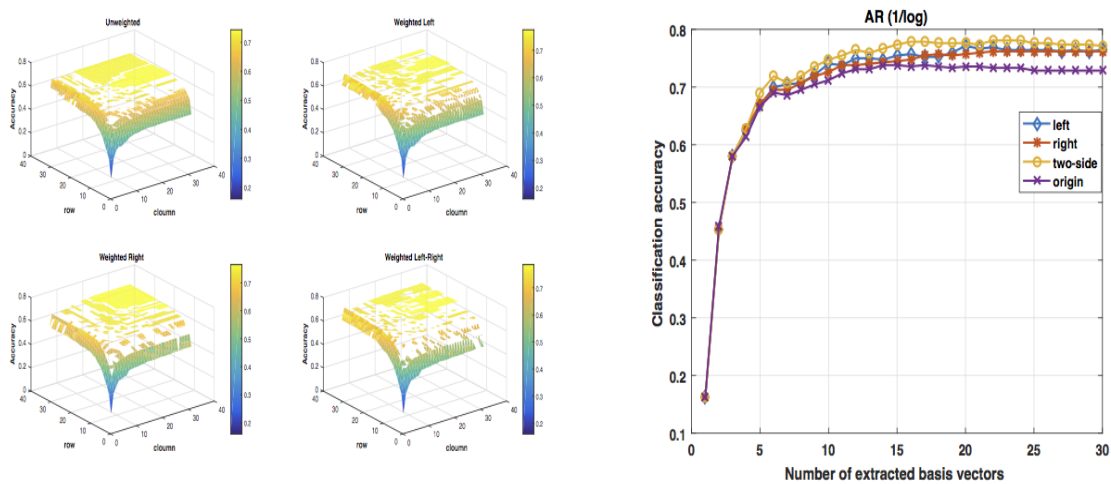


Figure 10: Recognition accuracies of BiG2DQPCA on the AR validation set with $f(W) = 1/\log(W)$.



Figure 11: Sample color face images from four rotated databases.

Acknowledgment

This work was jointly supported by National Natural Science Foundation of China, Grant nos. 12171210, 12090011, 11771188, and 61773384; the Major Projects of Universities in Jiangsu Province of China grants 21KJA110001; and the Natural Science Foundation of Fujian Province of China grants 2020J05034.

References

References

- [1] J. Yang, D. Zhang, A. F. Frangi, and J. Y. Yang, *Two-dimensional PCA: A new approach to appearance-based face representation and recognition*, IEEE Trans. Pattern Anal. Mach. Intell., 26(1) (2004) 131-137.

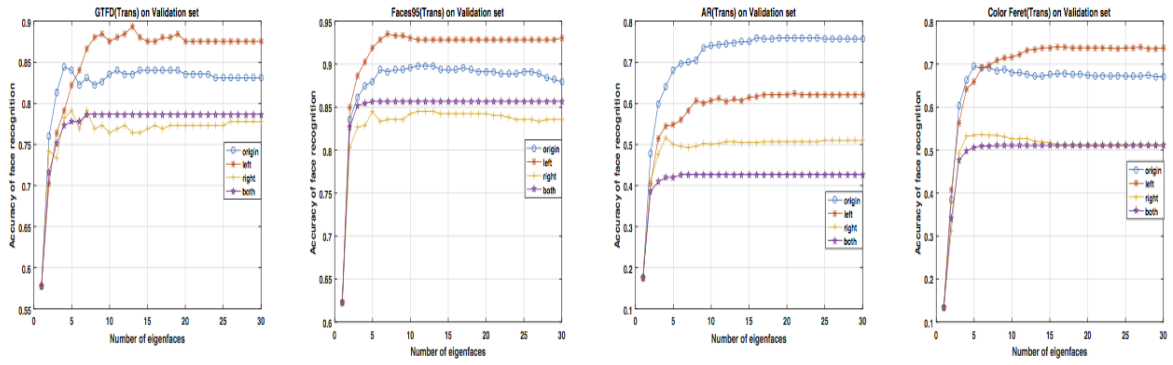


Figure 12: Recognition accuracies of BiG2DQPCA with four different weighing methods on the rotated GTFD validation set. The numbers of the chosen eigenfaces are from 1 to 30.

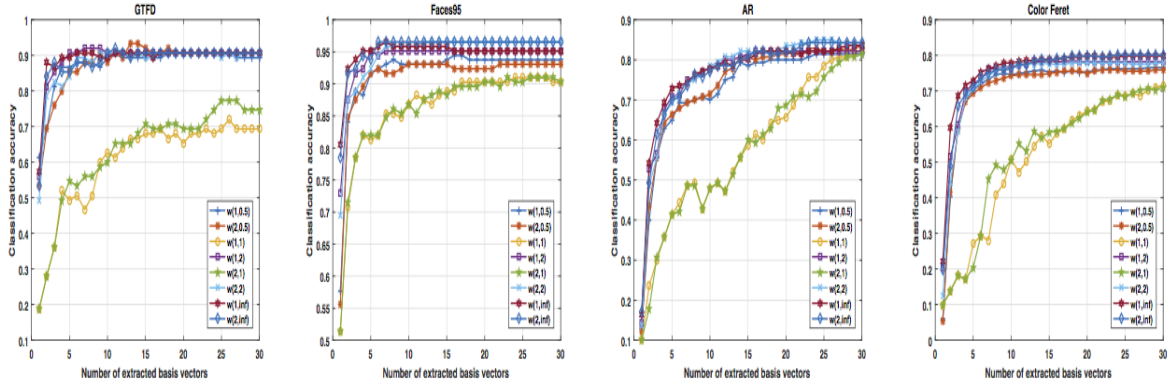


Figure 13: Recognition accuracies of BiG2DQPCA with different $w(s, p)$ on the four different databases.

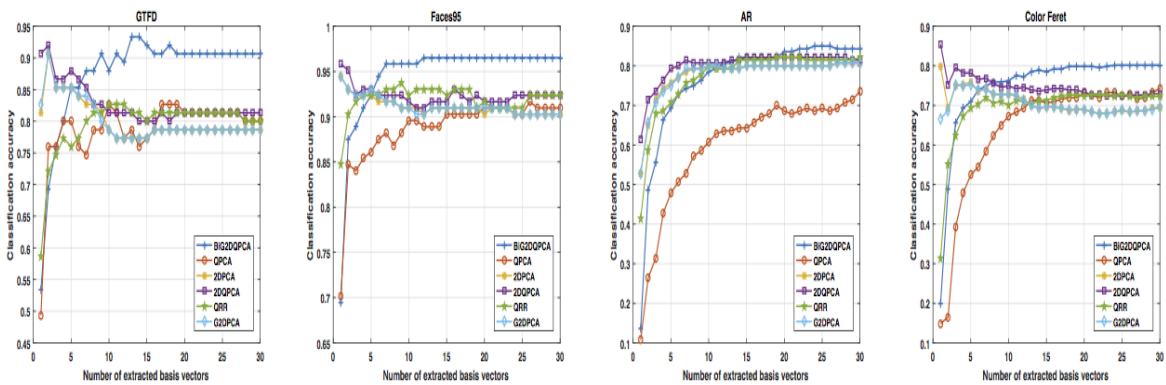


Figure 14: Face recognition rate of PCA-like methods for the different databases.

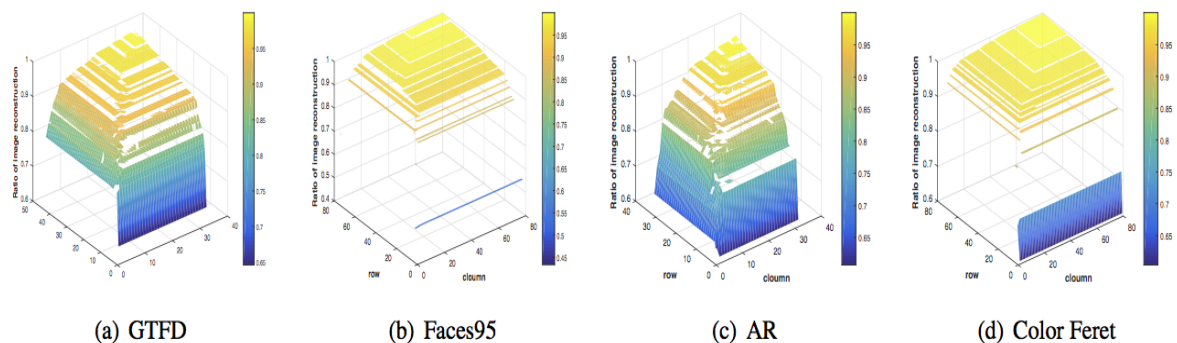


Figure 15: Ratio of the reconstructed images over the original face images on the four databases.

- [2] Y. Chen, X. Xiao and Y. Zhou, *Low-Rank Quaternion Approximation for Color Image Processing*, IEEE Trans. Image Process. 29(1) (2020) 1426-1439.
- [3] Z.-G. Jia, Q.-Y. Jin, M. K. Ng and X.-L. Zhao, *Non-local robust quaternion matrix completion for large-scale color image and video inpainting*, IEEE Trans. Image Process. 31 (2022) 3868-3883.
- [4] N. L. Bihan and S. J. Sangwine, *Quaternion principal component analysis of color images*, Proc. 2003 Tenth IEEE Int. Conf. Image Processing (ICIP 2003), 1 (2003) 809-812.
- [5] X. Xiang, J. Yang, and Q. Chen, *Color face recognition by PCA-like approach*, Neurocomputing, 152 (2015) 231-235.
- [6] Y. F. Sun, S. Y. Chen and B. C. Yin, *Color face recognition based on quaternion matrix representation*, Pattern Recognit. Lett., 32(4)(2011) 597-605.
- [7] B. J. Chen, J. H. Yang, B. Jeon and X. P. Zhang, *Kernel quaternion principal component analysis and its application in RGB-D object recognition*, Neurocomputing, 266(29) (2017) 293-303.
- [8] Z.-G. Jia, S.-T. Ling and M.-X. Zhao, *Color two-dimensional principal component analysis for face recognition based on quaternion model*, LNCS, 10361 (2017) 177-189.
- [9] Z.-G. Jia, M.-S. Wei and S.-T. Ling, *A new structure-preserving method for quaternion Hermitian eigenvalue problems*, J. Comput. Appl. Math. 239 (2013) 12-24.
- [10] Z.-G. Jia, *The Eigenvalue Problem of Quaternion Matrix: Structure-Preserving Algorithms and Applications*, Science Press, Beijing, Dec. 2019.
- [11] X. Xiao and Y. Zhou, *Two-Dimensional Quaternion PCA and Sparse PCA*, IEEE Transactions on Neural Networks and Learning Systems, 30(7) (2019) 2028-2042.
- [12] M. Zhao, Z. Jia and D. Gong, *Improved Two-Dimensional Quaternion Principal Component Analysis*, IEEE Access, 7 (2019) 79409-79417.
- [13] M. A. Turk and A. P. Pentland, *Face recognition using eigenfaces*, Proc. IEEE Conf. Comput. Vis. Pattern Recognit., (1991) 586-591.
- [14] Q. Ke and T. Kanade, *Robust L_1 norm factorization in the presence of outliers and missing data by alternative convex programming*, IEEE Conf. Comput. Vis. Pattern Recognit., San Diego, CA, USA, 2005, 739-746.
- [15] C. Ding, D. Zhou, X. He, and H. Zha, *R_1 -PCA: Rotational invariant L_1 -norm principal component analysis for robust subspace factorization*, Proc. Int. Conf. Machine Learning (ICML 2006), (2006) 281-288.
- [16] N. Kwak, *Principal component analysis based on L_1 -norm maximization*, IEEE Trans. Pattern Anal. Mach. Intell., 30 (9) (2008) 1672-1680.
- [17] S. Boyd and L. Vandenberghe, *Convex Optimization*, Cambridge university press, 2009.
- [18] H. Zou and T. Hastie, *Regularization and variable selection via the elastic net*, Journal of the Royal Statistical Society: Series B (Statistical Methodology), 67(2) (2005) 301-320.
- [19] H. Zou, T. Hastie and R. Tibshirani, *Sparse principal component analysis*, J. Comput. Graph. Stat., 15(2) (2006) 265-286.
- [20] H. Shen and J. Z. Huang, *Sparse principal component analysis via regularized low rank matrix approximation*, J. Multivar. Anal., 99(6) (2008) 1015-1034.
- [21] M. Journée, Y. Nesterov, P. Richtárik, and R. Sepulchre, *Generalized power method for sparse principal component analysis*, The Journal of Machine Learning Research, 11 (2010) 517-553.
- [22] F. R. On, R. Jäilani, S. L. Hassan and N. M. Tahir, *Analysis of sparse PCA using high dimensional data*, 2016 IEEE 12th International Colloquium on Signal Processing & Its Applications (CSPA2016), (2016) 340-345.
- [23] M. I. Razzak, R. A. Saris, M. Blumenstein and G. Xu, *Robust 2D Joint Sparse Principal Component Analysis With F -Norm Minimization For Sparse Modelling: 2D-RJSPCA*, International Joint Conference on Neural Networks (IJCNN), (2018) 1-7.
- [24] D. Meng, Q. Zhao, and Z. Xu, *Improve robustness of sparse PCA by L_1 -norm maximization*, Pattern Recognit., 45 (1) (2012) 487-497.
- [25] P. Peng, Y. Zhang, F. Liu, H. Wang and H. Zhang, *A Robust and Sparse Process Fault Detection Method Based on RSPCA*, IEEE Access, 7 (2019) 133799-133811.
- [26] Z. Liang, S. Xia, Y. Zhou, L. Zhang, and Y. Li, *Feature extraction based on L_p -norm generalized principal component analysis*, Pattern Recognit. Lett., 34(9) (2013) 1037-1045.

- [27] N. Kwak, *Principal component analysis by L_p -norm maximization*, IEEE Trans. Cybern., 44(5) (2014) 594-609.
- [28] X. Li, Y. Pang, and Y. Yuan, *L_1 -norm-based 2DPCA*, IEEE Trans. Syst., Man, Cybern. B, Cybern., 40 (4) (2010) 1170-1175.
- [29] J. Meng and X. Zheng, *Robust Sparse 2DPCA and Its Application to Face Recognition*, Symposium on Photonics and Optoelectronics, (2012) 1-4.
- [30] J. Wang, *Generalized 2-D Principal Component Analysis by L_p -Norm for Image Analysis*, IEEE transactions on cybernetics, 46(3) (2016) 792-803.
- [31] M.-X. Zhao, Z.-G. Jia, Y.-F. Cai, X. Chen, and D.-W., Gong, *Advanced Variations of Two-Dimensional Principal Component Analysis for Face Recognition*, Neurocomputing, (2021) online: <https://doi.org/10.1016/j.neucom.2020.08.083>.
- [32] J. Ye, *Generalized low rank approximations of matrices*, Mach. Learn., 61 (2005) 167-191.
- [33] D. Zhang and Z.-H. Zhou, *(2D)²PCA: Two-directional two dimensional PCA for efficient face representation and recognition*, Neurocomputing, 69(1) (2005) 224-231.
- [34] C.-N. Li, Y.-H. Shao, Z. Wang, and N.-Y. Deng, *Robust bilateral L_p -norm two-dimensional linear discriminant analysis*, Information Sciences, 500 (2019) 274-297.
- [35] Z.-G. Jia, Z.-J. Qiu and M.-X. Zhao, *Generalized Two-Dimensional Quaternion Principal Component Analysis with Weighting for Color Image Recognition*, arXiv:2010.01477.
- [36] D. R. Hunter and K. Lange, *A tutorial on MM algorithms*, The American Statistician, 58(1) (2004) 30-37.
- [37] S. C. Pei and C. M. Cheng, *Quaternion matrix singular value decomposition and its applications for color image processing*, Proc. 2003 Int. Conf. Image Processing (ICIP 2003), 1 (2003) 805-808.
- [38] X. Xiao, Y. Chen, Y. Gong and Y. Zhou, *2D Quaternion Sparse Discriminant Analysis*, IEEE Trans. Image Process., 29(1) (2020) 2271-2286.
- [39] J. Ye and Q. Li, *A two-stage linear discriminant analysis via QR decomposition*, IEEE Trans. Pattern Anal. Mach. Intell., 27(6) (2005) 929-941.
- [40] S. Noushath, G. Hemantha Kumar and P. Shivakumara, *(2D)²LDA: An efficient approach for face recognition*, Pattern Recognition, 39(7) (2006) 1396-1400.
- [41] Z. Liang, Y. Li and P. Shi, *A note on two-dimensional linear discriminant analysis*, Pattern Recognition Letters, 29(16) (2008) 2122-2128.